Stony Brook University

Properties of Boron Phosphide Films Grown on Different Substrates and Conoscopic Study of Sapphire

A Thesis Presented

by

Ruifen Chen

to

The Graduate School

in Partial Fulfillment of the

Requirements

for the Degree of

Master of Science

in

Materials Science and Engineering

Stony Brook University

May 2014

Stony Brook University

The Graduate School

Ruifen Chen

We, the thesis committee for the above candidate for the
Master of Science degree, hereby recommend
acceptance of this thesis.

Michael Dudley – Thesis Advisor
Professor, Department of Materials Science and Engineering

Balaji Raghothamachar – Second Reader
Research Professor, Department of Materials Science and Engineering

T.A. Venkatesh – Third Reader
Associate Professor, Department of Materials Science and Engineering

This thesis is accepted by the Graduate School

Charles Taber
Dean of the Graduate School

Abstract of the Thesis

Properties of Boron Phosphide Films Grown on Different Substrates

and Conoscopic Study of Sapphire

by

Ruifen Chen

Master of Science

in

Materials Science and Engineering

Stony Brook University

2014

Boron phosphide (BP) with its high capture cross section for thermal neutrons is potentially a great candidate material for neutron detectors. Bulk BP substrates are not readily available for developing detector devices therefor heteroepitaxial growth by CVD on commercially available substrates are currently being explored. The quality of BP films growth on commercial Si substrates is too poor for use in detector applications. In this thesis, we explore various substrates for suitability for BP heteroepitaxy by characterizing the crystalline quality of the epilayers grown under various growth conditions. Substrate materials used in this study include on-axis c-plane 6H-SiC, off-axis c-plane 4H-SiC with vicinal steps, Si substrates with 3C-SiC buffer layer and sapphire substrates with AlN buffer layers. Using SWBXT in combination with SEM and optical microscopy, we have compared the quality of BP grown on different substrates and the optimum growth condition and suitable substrates have been proposed. Also, the BP film growth mechanism and twin defect origination mechanism are explained based on experimental and theoretical studies. Based on experimental results, off-axis substrates could reduce the possibility of the presence of BP twin structure, but not sufficiently; the growth of BP film on Si substrates by

using 3C-SiC as a buffer layer has been exhibited as a preferable substrate, where no BP twin is revealed; for the growth of BP films on AlN/Sapphire substrates, poor quality of BP films and unknown materials are observed.

Sapphire is widely used as substrates for GaN-based LEDs for solid state applications and other related industries. High transparency and low defect density are desirable properties of sapphire wafers for these applications. However, undesirable defects in sapphire wafers hamper their development. Various characterization techniques are used to examine the quality of sapphire. In this study, by comparing conoscopic patterns with X-ray Topographs, actual defect distributions have been correlated with conoscopic patterns and the reliability of conoscopic results for evaluating the quality of sapphire wafers has been studied.

Table of Contents

List of Figures and Tables

List of Abbreviations

XRT	X-ray Topography
XRD	X-ray Diffraction
SWBXT	Synchrotron White Beam X-ray Topography
CVD	Chemical Vapor Deposition
SEM	Scanning Electron Microscopy
HRTEM	High Resolution Transmission Electron Microscopy
HEM	Heat Exchanger Method
EFG	Edged-defined Film-fed Growth

ACKNOWLEDGEMENTS

First I would like to give my sincerity gratitude to Professor Michael Dudley, my advisor, for providing me this great opportunity to study in the field of single crystal characterization. His wide knowledge and helpful guidance have been of great value for me. No doubt his understanding, encouragement and personal guidance have always been providing an excellent basis for my research.

I would like to thank Dr. Balaji Raghothamachar, valuable suggestion and discussion during the entire research project.

I would like to thank Professor T. A. Venkatesh for being in my committee member and his help and suggestion during my research project.

I would like to thank my colleagues: Mr. Fangzhen Wu, Ms. Huanhuan Wang, Dr. Shayan Byrappa, Ms. Hao Wang, Mr. Goue Ouloide Yannick, Ms. Yu Yang, Mr. Zheyu Li for their help during my research.

I would like to thank Dr. Jim Quinn for help with Scanning Electron Microscopy.

I would like to acknowledge continuous help and support of graduate program coordinator Ms. Shauntae Smith, and Ms. Chandrani Roy.

I would like to thank my boyfriend Zihao Ding, without his patience and attentive care, I would not be able to spend my happy two-year master period.

Finally, I would like to thank my parents Mr. Pengbo Chen and Mrs. Xinling Lu, for their great assistance during my study. Without them, I would not have been able to spend so much time on my research.

CHAPTER.I. INTRODUCTION

1.1 Background of BP

Solid State neutron detection technology has great potential in bringing discoveries in material science for developing semiconductor devices to support national security applications. However, few elements have a significant capture cross section for thermal neutrons, and among them, fewer still are the amount of elements that are suitable for constructing a solid-state semiconducting device and therefore have limited the development of neutron detector. Boron with its large capture cross-section and high performance in generating high-energy ions becomes a unique suitable semiconductor material for thermal neutrons. [1]

With excellent performance on the neutron cross-section (around 3840 barns), abundance, and chemical reactivity, ^{10}B in semiconductor detectors is preferred in comparison with ^{6}Li whose cross section is less than 1000 barns. Normally, two nuclear reactions will occur when ^{10}B reacts with thermal neutrons[2]:

$$^{10}B + n \rightarrow ^{7}Li\ (0.84\ MeV) + ^{4}He\ (1.47\ MeV) + \gamma\ (0.48\ MeV) \quad (94\%)$$

$$^{10}B + n \rightarrow ^{7}Li\ (1.02\ MeV) + ^{4}He\ (1.78\ MeV) \quad (6\%)$$

Both processes will create large enough charge, which can easily be detected with no amplification. This offers a great candidate for p-n junction or pin diodes, which brings the future of fabrication of thermal neutron detectors.

Developing heterostructures by using boron compound and other semiconductor materials is mainly presented to the designs of boron based neutron detectors, due to the undesired low travel range of single boron coated materials. Excellently stable material properties and a wide band gap are considered as ideal characteristics for semiconductor materials.[3] Cubic boron phosphide (BP) with an indirect band gap of 2.0ev satisfies this qualification. Its lattice constant is 4.538Å, which is similar to that of both 3C-silicon carbide (SiC) 4.36Å, and gallium nitride (4.51Å for cubic GaN). The small atomic radius of boron (0.82 pm) leads to the great stability advantage of BP, which caused larger orbital overlap and higher ionization energy. BP decomposes to boron sub-phosphide ($B_{12}P_2$) at elevated temperatures and low phosphorus pressures by losing phosphorus, even if it has high stability. Fig.I.1 illustrates the crystal structures of both boron phosphides.[2]

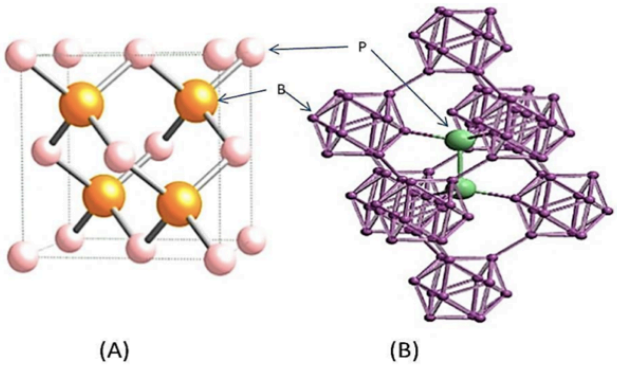

Fig.I.1 (A) Structure of cubic boron phosphide (B) Structure of boron subphosphide

The shortage, like low charge carrier mobility, high resistivity, and low thermal conductivity, makes boron sub-phosphide ($B_{12}P_2$) to be an undesired phase during BP synthesis. So, the factors, like temperature, gas pressure and flow rates, become the key to control with.

Currently, most research have successfully grown BP epilayer on substrates, like Si, GaN, sapphire and SiC by CVD method. The key factor that affects the quality of film is the mismatch between substrate and film. Because if the lattice constant mismatch between films and substrates becomes too large, the mosaic structures and other major defects will cause failure of the whole device. Based on several papers, the mismatch between BP (lattice parameter a=4.538Å) and Si (a=5.431Å), sapphire (a=4.785Å, c=12.991Å) is up to 17%, which is unsuitable for use as detectors. On the contrary, the mismatch will only be 4.5% for BP (111) plane and the close packed plane of SiC, which brings great potential to semiconductor devices, because SiC not only has good crystal structure with BP, but also has wide band gap, high electron mobility and high thermal conductivity.

The most widely used SiC polytypes are 3C-SiC, 4H-SiC and 6H-SiC, but since 3C-SiC is not commercially developed, 4H-SiC and 6H-SiC substrates are main focus of study here. Also, this study lists the comparison among the growth of other substrates, like 3C-SiC/Si and AlN/sapphire. Although the high mismatch between Si, sapphire and BP has result in lack of interest, using a buffer layer, like 3C-SiC or AlN, has attenuated this disadvantages to some extent. So, above all, to get a better and more comprehensive evaluation of different substrates, there are mainly four kinds of substrates focused on. Comparison between Si, sapphire and SiC will be mainly analyzed in this study. Below list the general properties of the materials involved in the dissertation (Tab.I-1.)[3]

Tab. I-1 General property of the materials used in the dissertation [5]

	BP	Si	3C-SiC	4H-SiC	6H-SiC	Al_2O_3
Crystal structure	FCC	FCC	FCC	HCP	HCP	rhombohedral
Lattice constant (Å)	4.54	5.43	4.36	a=3.07 c=10.05	a=3.07 c=15.11	a=4.757 c=12.983
Coefficient of Thermal expansion (10^{-6} K^{-1})	3.6	2.6	4.0	4.0	4.0	4.46 4.16
Thermal conductivity (W/cm·K) at 300K	4.0	1.5	3.6	3.7	4.9	4.0
Bond energy (eV)	2.9	2.3	3.5	3.5	3.5	-
Band gap at RT (eV)	2.1	1.1	2.4	3.2	3.1	-
Hole mobility (cm^2/Vs)	70	480	40	120	80	-

Motivation

Based on above discussion, BP film grown on SiC (4H-SiC or 6H-SiC) has great potential to improve the quality of semiconductor devices. According to the previous work on the structure difference of BP and SiC, the possible presence of twin defects and boron sub-phosphide ($B_{12}P_2$) will deteriorate electrical properties of devices. Thus the primary motivation of this study is to evaluate the quality of BP film, for example, checking whether the film is dominated by twin structures, and exploring the preferable substrates for epitaxial growth of BP films.

1.2. Introduction of Sapphire

Sapphire (a-Al2O3), which is widely used as substrate for GaN-based LEDs and other specialty industrial markets, has excellent characteristics, in particular high-hardness, chemical resistance, thermal conductivity and transparency. The structure of sapphire is formed by O^{2-} ions, which is closest packed hexagonal arrangement, and Al^{3+} cations filling two thirds of octahedral interstices between the closely packed O^{2-} ions (Fig.I.2). Sapphire belongs to rhombohedral or triangle system and the space group is $D_{3d}^6 - R3c$. [4]

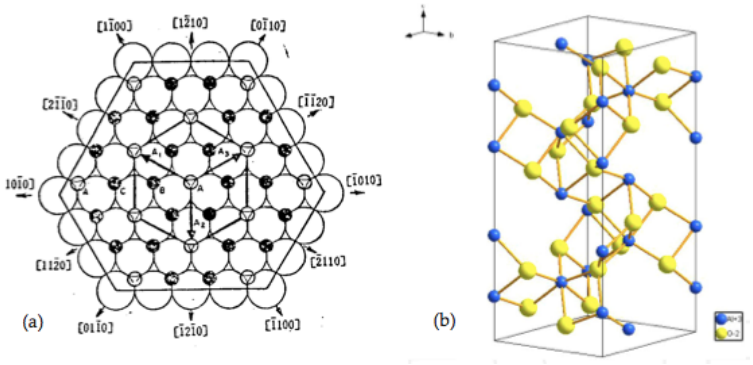

Fig.I.2 (a) Schematic of the packing of O^{2-} ion in the sapphire cell; (b) Rhombohedra unit cell of sapphire crystal

To get a high quality sapphire, the properties, such as transparent, free of bubbles, inclusions, twins, grain boundary, should be achieved by the seed crystal, because the quality of seed will severely affect the quality of crystal boule. If the seed contains stacking faults or grain boundaries, it will extend to the crystal boule and spread all over the whole boule, then lead to loss of yield. Normally, the growth direction is usually along a-axis[11-20], m-axis[10-10] or r-axis[1-102] directions to reduce subgrains and twin defects. And there are several ways to improve mechanical properties of sapphire, like carbon doping or titanium doping, which has been proven to be a good solution. The major physical property of sapphire lists in Tab.I-2.[4]

Tab. I-2 The major physical property of sapphire

Chemical Formula	**Al_2O_3**
Structure	Hexagonal- rhombohedral
Molecular weight	101.96
Lattice Constants Å	a=4.765, c=13.000
Crystal density (g/cm^3)	3.98
Melt density (g/cm^3)	3.0
Melting Point (°C)	2050
Thermal coefficient of linear expansion at 323 (K^{-1})	$66.66*10^{-6}$parallel to optical axis $5*10^{-6}$ perpendicular to optical axis

Thermal conductivity (W/m°K) at 20°C	41.9
Transmission Range	0.2-5.5 microns

The growth method of sapphire for this study is a type of Heat exchanger method (HEM). The principle of HEM is, by adjusting the heat exchange medium's (helium) flow rates, the crystal growth process can be controlled. When part of the seed is melted, to start crystallization of melt onto the seed, the flow rate is increased. However, both the temperature of flow will be decreased when the crystallization is complete, so the sapphire boule can be slowly annealed. (Fig.I.3)

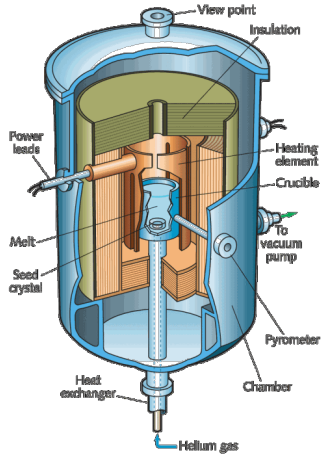

Fig. I.3 The schematic of HEM furnace

The heat exchanger method sapphire furnace has producing high quality sapphire that used in LEDs or other related industry areas. The sapphire is grown in low thermal gradient and low stress atmosphere, which make the production of high quality sapphire crystal possible.

Also, edged-defined film-fed growth (EFG) method is widely used in recent years. For this technique, special used crystal, like ribbon and tuba-shaped, can be produced, which brings great opportunity in shaped crystal market. The growth principle of EFG furnace is, due to capillarity, the melt rises to the top and forms a thin film layer, then spreads to the surrounding; meanwhile, the crystallization of the seed is formed. Depend on this growth principle, EFG furnace has many advantages, like low cost, fast growth rate and multiple shape crystal can be obtained. But this technique can also nucleate crystalline, like grain

boundaries, dislocations, and residual stress. Below exhibits the schematic of EFG furnace (Fig.I.4).

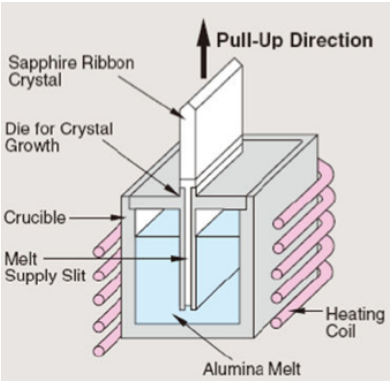

Fig. I.4 The schematic of EFG furnace

Motivation

Since sapphire is an important material for electronic and other application, because of its favorable electrical and mechanical properties, so obtaining a high quality and large size sapphire crystal has been an important topic. HEM growth method has the advantage of growing large size and high-quality sapphire crystal along c direction. Therefore, to get a better idea of the quality of sample, this study described and analyzed the major defects of sapphire by optical method and x-ray topography method (Acknowledge work of Jianqiu Guo in acknowledgement section).

CHAPTER.II. RESEARCH METHODOLOGY

2.1. Synchrotron White Beam X-ray Topography

X-ray topography (XRT) is a nondestructive method that used in single crystal's characterization. The application of synchrotron white beam X-ray topography (SWBXT)[23] is focused on various crystal defects observation and analysis. Through X-ray topography method, Burgers vectors, line direction of dislocations, inclusions and other valuable information can be obtained by analyzing the contrast variations.

Normally, the individual spots obtained from Laue diffraction patterns from crystals do not have uniform contrast. The basis for the X-ray topographic technique is due to the structural uniformity in the lattice planes, the diffraction spot with localized variations in the intensity is formed. Local changes in orientation and spacing of crystal lattice planes cause local differences in either diffracted beam direction or intensity, which means, under appropriate experimental conditions, are manifested as observable contrast on X-ray topography.[5] In general, there are two basic mechanisms for contrast; one is orientation contrast caused from subgrains and twins (Fig.II.1.), the other is extinction contrast that arises when the scattering power around the defects differs from that in the rest of the crystal.

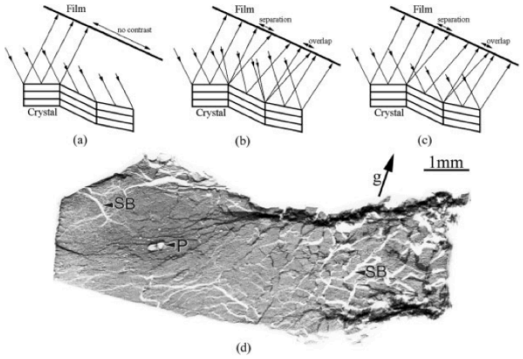

Fig.II.1 Orientation contrast from misoriented regions: (a) beam divergence<misorientation; (b) beam divergence>misorienctation; (c) continuous radiation; (d) Reflection topography from an HgCdTe single crystal.

Generally, the widely used systems in X-ray topography are transmission, back reflection and reflection that differs in sample holding type, the arrangement of sample and photographic film. (Fig.II.2) In transmission system, the information of whole bulk material can be observed, which is caused by x-ray beam passing through the sample, while in

reflection geometry, based on its low penetration depth, only the surface information can be collected. In this study, these two geometries are commonly used. The synchrotron X-ray beam used in this study is at beamline X19C, NSLS, Brookhaven National Lab.

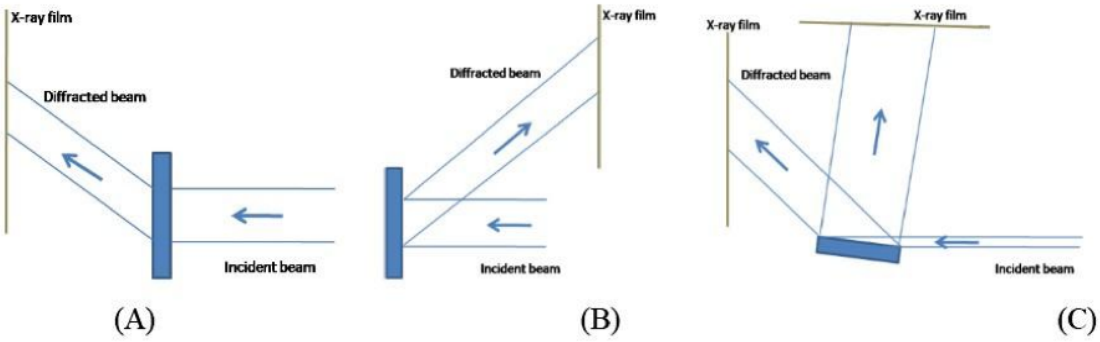

Fig. II.2 (A) Transmission System; (B) Back-reflection System; (C) Reflection System

Since the source is x-ray white beam, which means it contains a wide range of x-ray wavelengths, so, unlike normal X-ray diffraction (XRD) where only one diffraction plane is active at a time, white beam x-ray topography forms a whole diffraction pattern from multiple crystal planes. The image can be found in Fig.III.2. In this study, the diffraction pattern is critical to determine the twin defect of BP epitaxial layers. Twin can be classified into two types, one is growth twin, formed by a change of lattice during the crystal growth, and deformation twin, which is caused by mechanical stress. In this thesis, the growth twin is main type present in BP epitaxial layers. To better understand this, the stereographic projection of twin boundaries needs to be discussed.

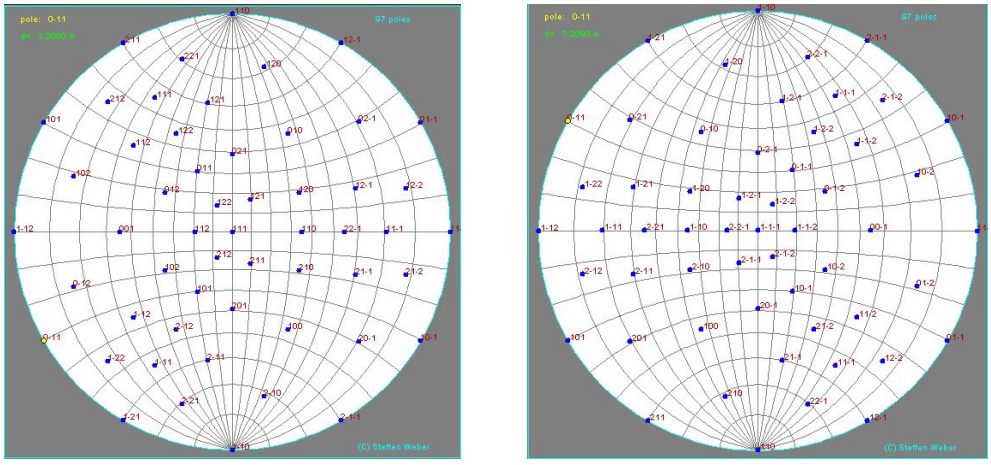

(a) (b)

Fig. II.3 Images are captured from Jcrystalsoft (a) (111) matrix stereographic projection; (b) (111) twin stereographic projection

The stereographic projection is a graphical method to exhibit the angular relationships between different planes on a two-demission paper. The orientation of plane is usually represented by its normal. For the projection of (111) plane of FCC structure, the relative position of each spot is constant on the stereographic projection. And since the twin is formed by 180° rotation about mirror plane, so, the 180° rotation of matrix projection will get the projection of the twin regions. Therefore, during the SWBXT experiment, the diffraction pattern will include both the matrix's pattern and the twin's pattern, rotated by 180° compared to matrix (Fig.II.3).

When dealing with thick sample or the surface information characterization, the penetration depth, which is defined as the depth (t) at which intensity drops to 1/e, helps in understanding the defect configurations information, because it shows the crystal volume imaged.

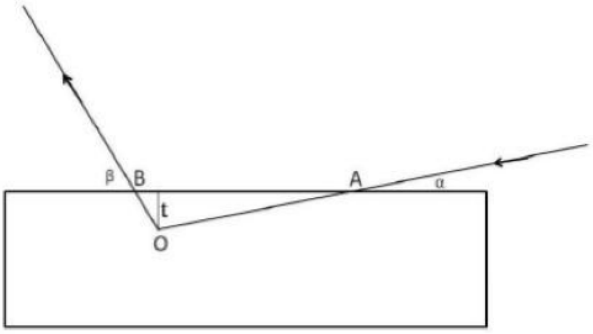

Fig. II.4 The schematic of penetration depth in reflection geometry

Fig. II.3. shows the schematic of penetration depth. AO represents the incident beam path in the crystal, BO represents the exit beam path and AB shows the surface of crystal. Then, based on above information, AO and BO could be written as,

$$AO = \frac{\mathrm{t}}{\sin\alpha}, OB = \frac{t}{sin\beta}$$

Total path lengths that x-ray pass through the crystal:

$$\tau = OA + OB = \frac{t}{sin\alpha} + \frac{t}{sin\beta}$$

The absorption effect of x-ray:

$$\frac{I}{I_0} = e^{-\mu\tau}$$

The definition of penetration depth:

$$e^{-\mu\tau} = \frac{1}{e}$$

Therefore, based on

$$\mu\tau = 1$$

$$\mu\left(\frac{t}{sin\alpha} + \frac{t}{sin\beta}\right) = 1$$

the penetration depth

$$t = \frac{1}{\mu\left(\frac{1}{sin\alpha} + \frac{1}{sin\beta}\right)}$$

where μ is absorption coefficient, α represents the incident beam angle with surface, β is the exit beam angle with the surface.

Above all, the SWBXT technique is an outstanding method in defects analysis, like dislocation density calculation, stacking faults and micropipes evaluation. And also, the synchrotron white beam x-ray offers great advantages in higher resolution and deeper penetration depth. By using this method, most characterization of crystal has been analyzed.

2.2. SEM

Scanning electron microscopy (SEM), which belongs to electron microscopy, produces high-resolution images by scanning sample with a focused beam of electrons. When electron beam interact with atoms in the sample, various signals emitted, which can be used in surface morphology analysis and composition identification.

The most widely used type of detection is secondary electrons, backscattering electrons and characteristic x-rays (Fig.II.4). The secondary electrons are formed when the incident electron beam excites the outer shell electrons of atoms, and only electrons from a few nanometers below surface can emit. Therefore, secondary electrons signal can well define the surface morphology of sample.[6] The backscattering electrons are generated

when incident electrons elastic scattering interaction with specimen atom nucleus, due to the difference in nucleus weight of variant chemical, both physical and chemical characteristics of the sample can be recorded. And the characteristic x-ray is created when the inner shell electrons have been kicked out by incident beam, then to remain stable, the outer shell electrons fill the inner shell, the energy difference between the two level will emit as x-ray, which is named as characteristic x-ray. Based on the formation principle of these three signals, the secondary electrons are used in surface morphology analysis, and backscattering electrons and characteristic x-ray can be used in composition analysis, because the signals are related to atomic number. For this study, the surface morphology is more important in studying twin structures, so secondary electron signals detector will be utilized.

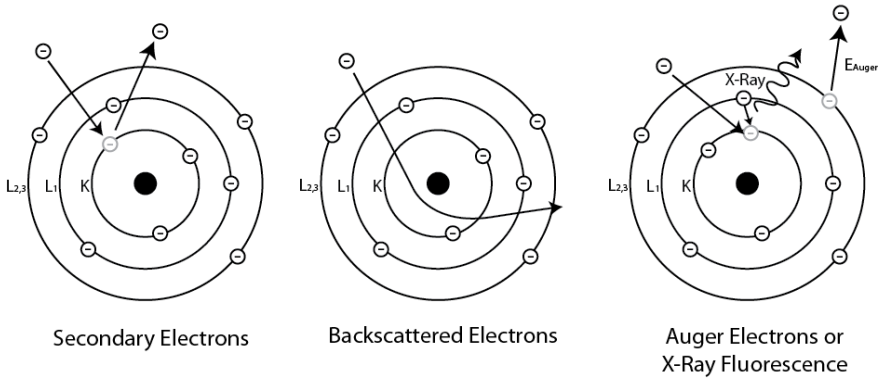

Fig. II.5 Scattering mechanisms of secondary electrons, backscattering electrons and X-ray fluorescence

For this study, the SEM instrument model is LEO1550, which is a high performance Schottky field emission SEM with a resolution of 5-10nm depending on the sample type.[7]

2.3. Polarized Optical Microscopy

The optical microscopy has been widely used in solid-state analysis, ranging from simple shape describe to crystallography analysis. The appearance of polarized optical microscopy has extensively extended the application range, like it offers the possibility in obtaining crystallographic information on small crystals and internal structure image with colors.

The properties, like wavelength, intensity, polarization and phase, for all the electromagnetic radiation, including visible light, are same. And polarization means there exists limitation in wave oscillation direction. The polarized optical microscopy has two major components: polarizer and analyzer. The polarizer is the first filter that only allows

one oscillation direction to pass, and the analyzer is the second filter that works the same way as polarizer, but these two components have relative angle difference. Normally, for the formation of Maltese cross patterns in single crystals, the angle is 90°. Maltese cross interference figure will be formed when the materials with two vibration directions, on the other side, for materials with three vibration directions, such as triclinic and monoclinic, the hyperbola type interference figure will formed (Fig.II.5).

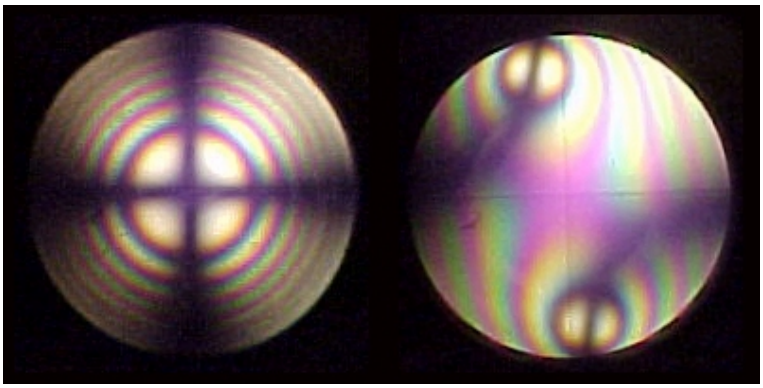

(a) (b)

Fig. II.6. (a) Maltese cross formed by materials with two vibration directions; (b) Hyperbola interference pattern formed by materials with three vibration directions

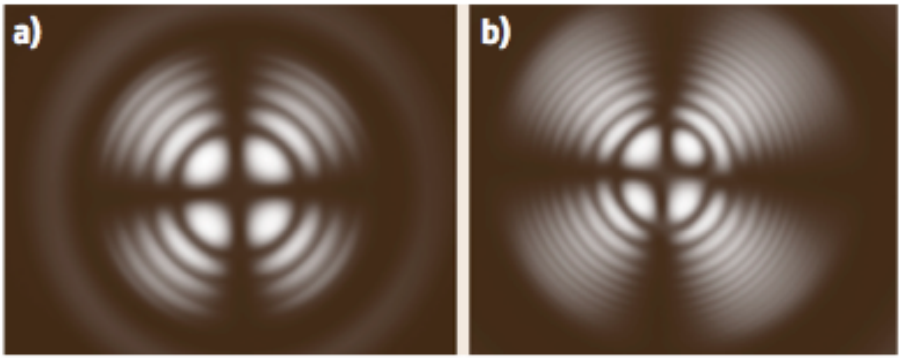

Fig. II.7 (a) Conoscopic pattern of high-quality sapphire. (b) Conoscopic pattern of sapphire ingot that has a few low-angle boundaries

The model of polarized optical microscopy used in this study is Nikon Eclipse E600, which is an optical microscopy with polarized light. The Maltese cross interference figure, which is achieved by polarized light microscopy, is a simple optical tool for analyzing optical inhomogeneity from very small crystals to large-size boules, which shows the overview quality of the sample. A perfect cross and four segments in symmetrical circular pattern of dark and bright fringes will be observed if the sample has low defect density

(Fig.II.6), otherwise, the distortion of fringes can be revealed. This method can only show the dislocation density relatively. Generally, this method can reveal the misorientations, grain boundaries, block structures and the stress levels.

In this study, conoscopic pattern has been used to evaluate the quality of sapphire wafer and show the fringe changes around grain boundaries.

2.4. Chemical Vapor Deposition (CVD)

One of the common methods for BP film grown on SiC is chemical vapor deposition (CVD), because of the high phosphorus vapor pressure under melting temperature, synthesizing bulk crystalline BP is difficult to achieve. The thin BP film can be formed by either using thermal decomposition of B_2H_6 and PH_3 in a hydrogen atmosphere or by using the thermal reduction of BBr3 and PCl3 mixtures with hydrogen gas. The reaction equation shows below.[2]

$$B2H6 + 2PH3 \xrightarrow{Heat} 2BP + 6H2$$

$$BBr3 + PCl3 + 3H2 \xrightarrow{Heat} BP + 3HBr + 3HCl$$

For the first method, the reactants, B_2H_6 (1% in H_2) and PH_3 (5% in H_2), are filled into a tube chamber leading to BP deposited on a substrate. By controlling temperature, pressure, flow rate ratio and substrate types, the quality of BP film can be adjusted. For the second method, the carrier gas is bubbled through two constant temperature bubblers containing liquid BBr_3 and PCl_3. Fig.II.7 shows the basic structure of CVD instruments for growing BP film.

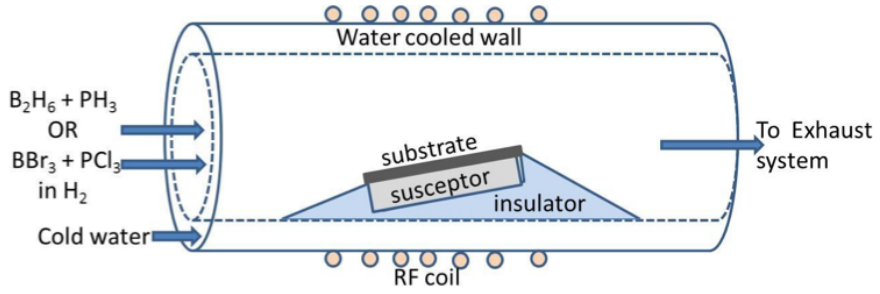

Fig. II.8 Schematic illustration of a CVD reaction chamber

For this study, the BP samples were grown by the research group led by Professor James Edgar at Kansas State University, under different growth condition.

CHAPTER.III.EXPERIMENTAL RESULTS AND ANALYSIS

3.1. Defect Study of Epitaxial BP grow on SiC, 3C-SiC/Si and AlN/Sapphire

3.1.1. Characterization of epitaxial BP grown on on-axis c-plane 6H-SiC

Outline

An analysis of BP epitaxial layer grown on (0001) 6H-SiC substrates is studied by SWBXT, optical microscopy and SEM methods. And the twin and matrix features have dominated the BP epitaxial layer. The epitaxial relationship has been determined by SWBXT, which is $(111)_{BP}$<1-10>$_{BP}$||$(0001)_{6H\text{-}SiC}$<11-20>$_{6H\text{-}SiC}$.

Introduction

By using CVD method, the thin BP films have deposited on the (0001) 6H-SiC substrates. With previous knowledge of the structure of BP and 6H-SiC, the possible structural variants need to be considered, because the growth of lower symmetry materials on the higher symmetry materials always lead to some crystalline defects. And although the mismatch between SiC and BP is small enough, the lattice constant difference still will cause residual stress. When applying SWBXT method to analyze, the relative intensity of each diffraction spot should be discussed in detail, because the crystal structure may contain some point defects, which lead to the inconsistency of Laue pattern intensity. All the possible reason causing structural variants need to be analyzed and optimized.

Results and discussion

The optical microscopy and SEM shows the BP layer surface morphology and due to the thickness of BP epilayer and some contamination, the twin pattern does not show out clearly, but we can still observe two kinds of triangle which are relatively rotated by 180° about (111) BP surface normal (Fig.III.1). And the SWBXT marked the orientation of each layer and also exhibits some blurred spots, due to which coming from the high interfacial stress in the film (Fig.III.2).

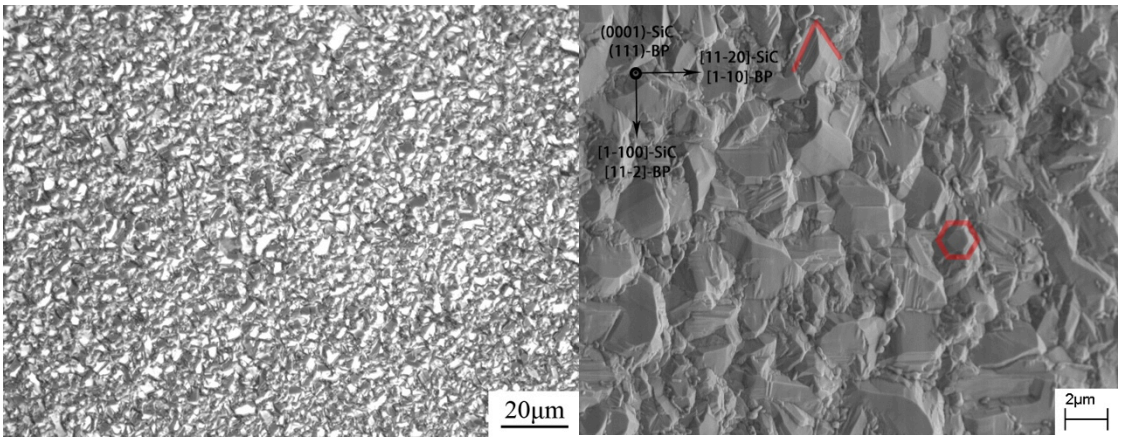

(a) (b)

Fig. III.1 (a) optical image of BP epilayer; (b) SEM image of BP layer

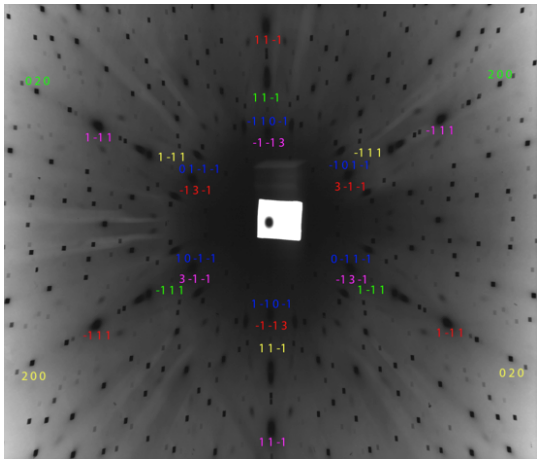

Fig. III.2. The SWBXT image and marked materials Laue pattern: blue represents 6H-SiC (0001); Red represents BP (11-1); Purple represents BP (11-1) twin; Green represents $B_{12}P_2$ (200); Yellow represents $B_{12}P_2$ (200) twin

Fig.III.1 shows the surface morphology of (111) BP epilayer. From SEM image, chemical liquids have contaminated the sample, which is caused by the organic liquid balls sitting between the valleys and blurring the original sharp cliff. However, it still exhibits some triangle features and a hexagonal shape, which proves the existence of twin structure to some extent.

Fig.III.2 shows the Laue pattern marked different materials present: blue represents 6H-SiC (0001); Red represents BP (11-1); Purple represents BP (11-1) twin; Green represents $B_{12}P_2$ (200); Yellow represents $B_{12}P_2$ (200) twin. Based on the high contrast of blurring spots, the interfacial strain between BP and 6H-SiC is quite large. Also the Laue pattern shows the presence of boron sub-phosphide, which as mentioned before is formed

by decomposition of BP at elevated temperatures and low phosphorus pressures by losing phosphorus. Due to its low charge carrier mobility, high resistivity, and low thermal conductivity, the presence of $B_{12}P_2$ is undesirable.

Since the presence of BP twin and boron sub-phosphide has been confirmed in the BP epilayers, detailed analysis of crystal structure and the bonding configuration should be analyzed. (Fig.III.3) The structure has been built by CrystalMaker software. Based on the Fig.3.1.1-3, the six-fold symmetry configuration of 6H-SiC has been revealed, which offers the possibility of BP bonding structural variants.

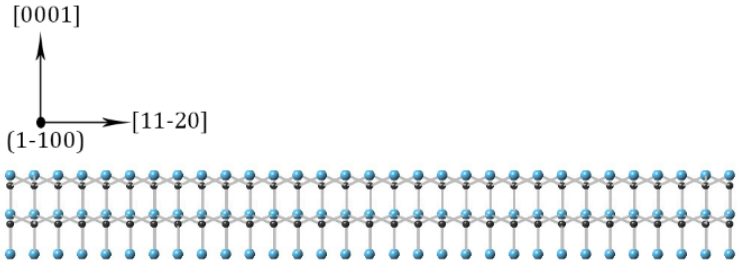

(a)

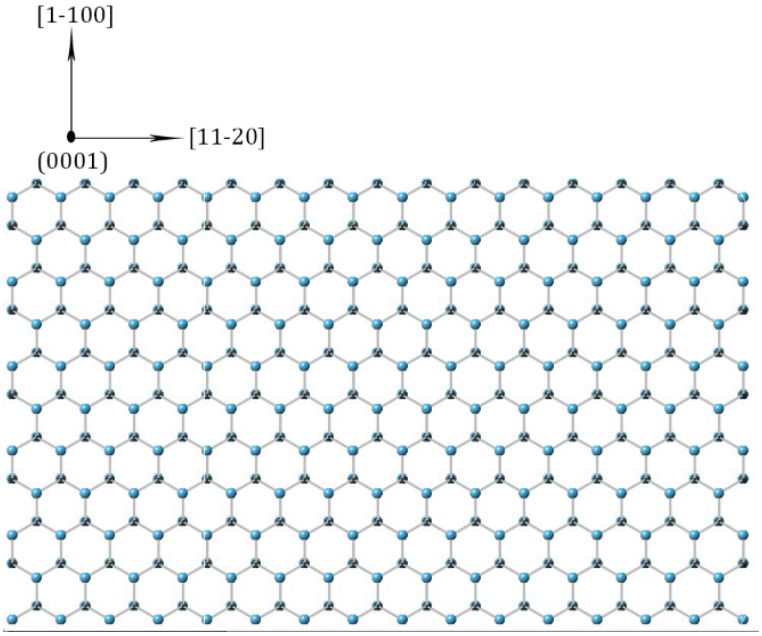

(b)

Fig. III.3. (a) the (1-100) plan view of 6H-SiC; (b) the (0001) plan view of 6H-SiC

To better understand how to connect BP with 6H-SiC, the bonding configuration has been described by Fig. III.4. The three dangling bonds of boron atoms connect with silicon atoms, as it shown in figure, there are at least two ways to bond. The two bonding ways are pointing to the opposite direction, which forms the growth twin defects.

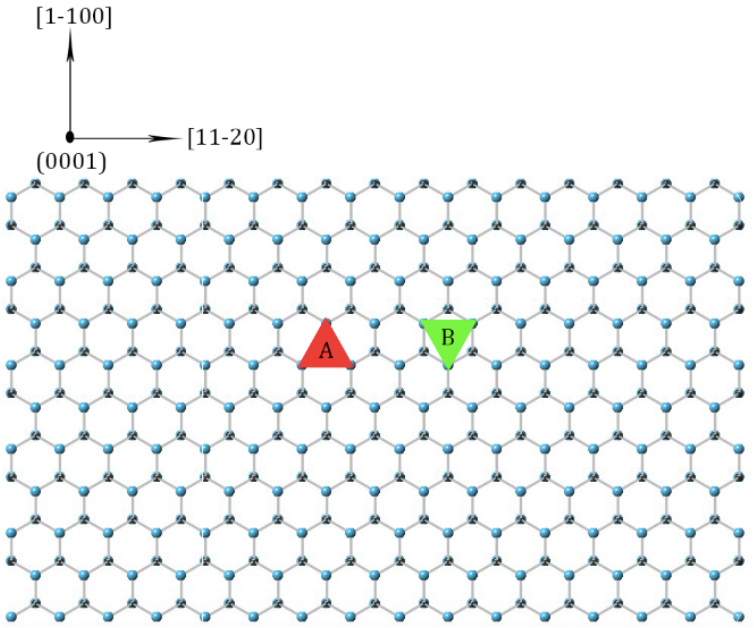

Fig. III.4 The bonding configuration illustrated BP and 6H-SiC

In the Fig.III.4, the bonding configuration shows that three boron-dangling bonds of BP connect to c-plane 6H-SiC. Position A and B explain the reason of appearance of growth twin, which is, the platform is wide enough for BP to bond with, so narrowing the terrace will be a choice to eliminate the twin defects.

Conclusions

BP epitaxial layer grown on c-plane 6H-SiC substrate is characterized by optical microscopy, SWBXT and SEM technique. The growth orientation is $(111)_{BP}<1\text{-}10>_{BP}||(0001)_{6H\text{-}SiC}<11\text{-}20>_{6H\text{-}SiC}$. Twin BP dominates the BP layer, which can potentially cause device failure. By detailed analysis of the structure of both films and substrates, the possible bonding configuration has been built and there exists multiple choice for BP to sit on, which lead to the formation of twin defects in BP layer. To solve this problem, narrowing the terrace width of 6H-SiC or changing to other substrates need to be examined.

3.1.2. Characterization of epitaxial BP grown on 4.37° off-cut 4H-SiC

Outline

The epitaxial BP layer grown by CVD on 4.37° off-cut along [1-100] 4H-SiC substrate is studied by optical, SWBXT, SEM method. It shows that the obscure presence of twin structure. The epitaxial relationship is BP grown on c-plane 4H-SiC, which is $(111)_{BP}<1\text{-}10>_{BP}||(0001)_{4H\text{-}SiC}<11\text{-}20>_{4H\text{-}SiC}$.

Introduction

Based on prior discussion in structure of BP and SiC, when a three-fold symmetry layer grown on a six-fold symmetry substrate, a mixture of structure variants is easy to happen. And when substrate has a single terrace, the boron phosphide films can grow in various orientations with equal chances, which lead to the domination of twin boundaries and mosaic structures. Therefore, to solve this major defect in thin film growth, breaking up the single terrace of substrate into a series of terrace should be a choice, since it diminishes the symmetry level and reduces the terrace platform area. The key problem turns out to be the degree of off-cut angle, which should vary within a range. If the off-cut angle is too large, then the bonding energy between relative steps will be out of reach, which leads to the break down of materials. On the contrary, if the off-cut is too small, the terrace will be large enough for all possible orientation to grow. So, in this study, multiple off-cut angle have been analyzed and compared, by now, the best off-cut angle for BP epilayer grown on 4H-SiC is 4.37° along [1-100].

Results and discussion

The off-cut angle, which is 4.37° along [1-100], has been measured by using SWBXT method and laser instrument (Fig.III.5). Fig.III.7 shows the optical image and SEM image from local area on the surface of BP layer. It shows two kinds of triangular features, which point along the [1-100] direction, and they are relatively rotated by 180 degree around [111] BP surface normal. These features reveal that the domination of twin structure in BP layers. SWBXT technique can be used to determine the orientation of BP (Fig.III.6).

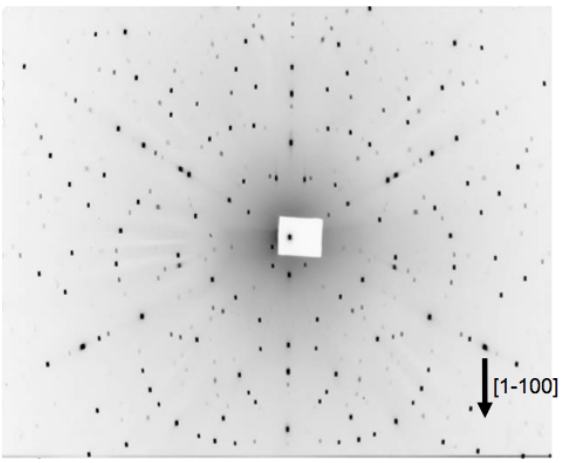

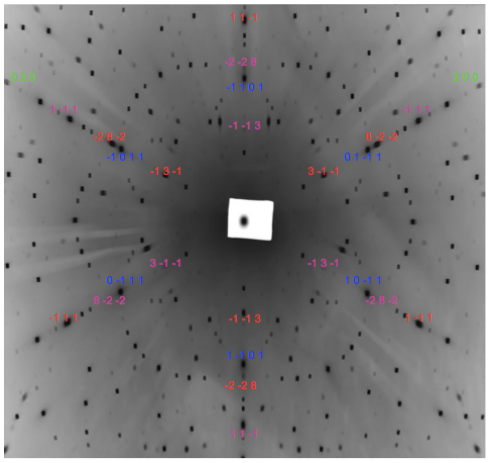

Fig. III.5. SWBXT measured off-cut angle 4.37° Fig. III.6 The laue pattern of sample, blue represents 4H-SiC

In Fig.III.6, the blue represents diffraction spots from 4H-SiC; Red represents BP (11-1); Purple represents BP (11-1) twin; Green represents $B_{12}P_2$ (200). The blurred spots, which is relatively rotated by 180° about matrix BP diffraction pattern, proved the existence of twin.

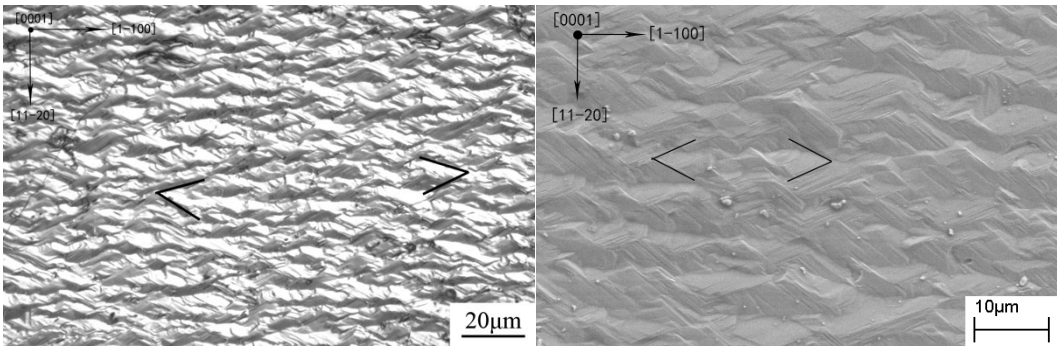

Fig. III.7. Optical image and SEM SE2 image of BP epilayer shown the two kinds of triangle pattern

Based on the information above, the BP layer is dominated by twin structure and the boron subphosphide ($B_{12}P_2$) spots appear in the Laue pattern. To explain the reason why the structural variants appear in the epilayer, the structure of substrate with an off-cut angle is analyzed (Fig.III.8).

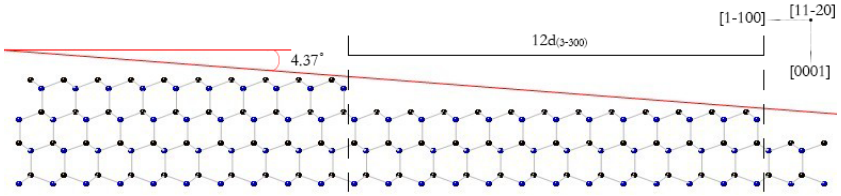

(a)

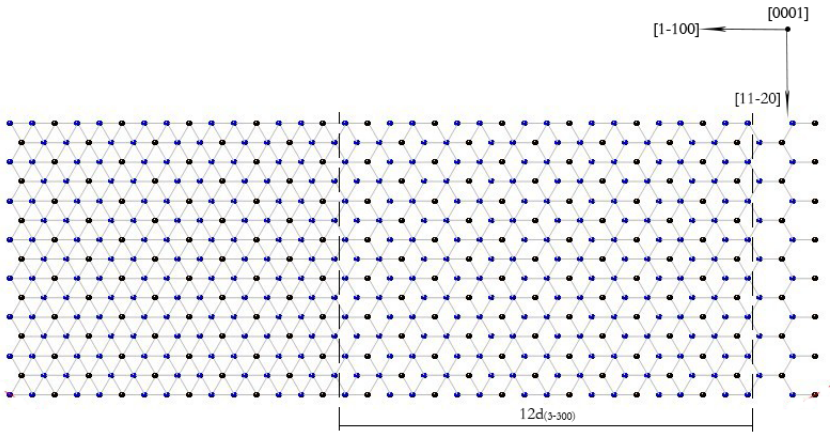

(b)

Fig. III.8 (a) The (11-20) plan view of 4H-SiC substrate with the periodic terrace. (b) Plan view of 4.37° off-cut c-plane 4H-SiC substrate surface

Depend on the structural image above, to get the 4H-SiC substrate with an 4.37° off-cut angle, a series of atomic steps should be arranged. Assuming each step riser is one SiC bilayer height, then to accomplish the 4.37° angle, the width of each terrace should be 12 layers that each layer is spaced by (3-300) planes.

For the growth of BP, the possible nucleation way is BP deposited on each terrace of 4H-SiC substrate. Since the Si triangular bond configuration is quite suitable for boron atom to bond, for which and the misfit between substrate and epilayer is 4.42% (d_{Si}=3.073 Å, d_B=3.209 Å), and the Si face is six-fold symmetry in c-plane while the BP is three fold symmetry in (111) plane, so the possible position for BP to bond with SiC can be multiple (Fig.III.9). The configuration of phosphide atoms bonded with Si can be in position A, or with a rotation of 180° around [111] BP axis in position B. These two kinds of arrangement structure describe the principle of the presence of twin structure in BP layer. The off-cut angle of 4.37°, which means the width of terrace is 12 layers, is still wide enough that all these two kinds of configuration can be happened at the same time, which caused the structural variants in the BP film.

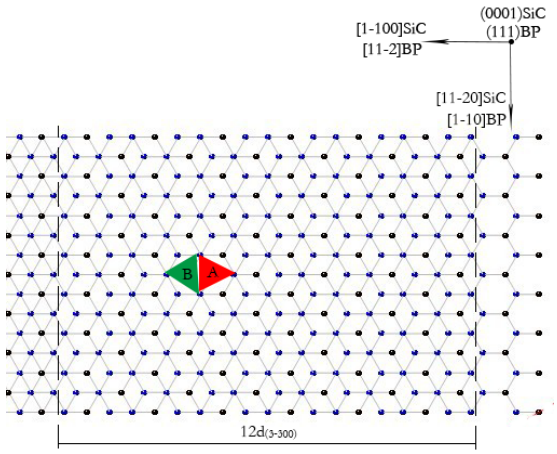

Fig. III.9 Plan view of two possible rotationally variant nucleation sites (A, B) for BP in twinned orientation

Also, other information we can obtain from SWBXT is the relative intensity difference. But because the diffraction spots are present from the whole sample, intensities of some spots may be the overlap of different materials, which lead to the different relative intensity compared to standard Laue pattern. Therefore, to analyze the main effect of each spot, detailed comparison among standard Laue pattern and photographic films has been analyzed below (Fig.III.10). The major spots intensity difference is exhibited from BP layer, where some high intensity spots appear weak while some low intensity spots appear strong contrast.

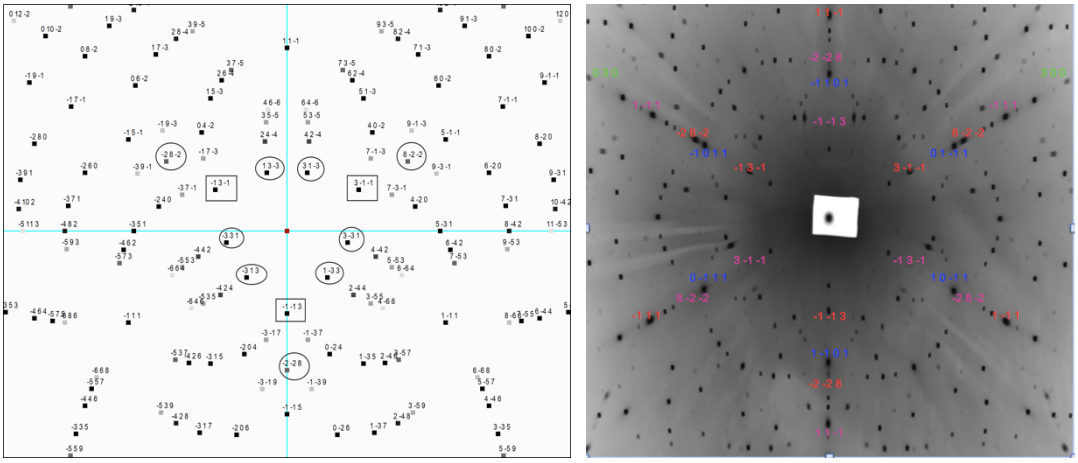

(a) (b)

Fig. III.10 (a) (111) BP<1-10>BP; (b) the symmetry pattern got from x-ray topography

For detail description, first, the three spots (relative intensity = 1605.656) marked in square are diffraction spots from BP, which show high contrast in simulated pattern. But for twin BP spots, which represent in pink color in Fig.III.10 (b)((-1 -1 3), (3 -1 -1), (-1 3

-1)), the contrast are pretty weak that means the ratio of twin BP is low. That is to say, although this sample has twin structure, but overall, the matrix BP dominates the epitaxial layer.

By comparing the standard Laue pattern's relative intensity with the real sample's, some inconsistencies have been found out. For example, the standard relative intensity of spots (-2 8 -2) and (8 -2 -2) should be 5.972, which is extreme weak, but in the SWBXT image, the contrast appears as strong as (-1 3 -1). At the same time, in principle, the intensity of (-2 -2 8) should be same as (-2 8 -2), but it appears as a weak spot, not like (-2 8 -2). The reason for this inconsistency may be caused by antisite point defect, which occurs when atoms of different type exchange positions. For example, in principle, boron atoms sit in four positions, which are (0 0 0), (0.5 0.5 0), (0.5 0 0.5) and (0 0.5 0.5), and phosphide atoms sit in other four positions, which are (0.25 0.25 0.25), (0.75 0.75 0.25), (0.75 0.25 0.75) and (0.25 0.75 0.75). However, the crystal structure cannot be always perfect, which means the exchange of position between B atoms and P atoms will happen easily. If that is the case, the relative intensity of diffraction Laue pattern will change simultaneously. To identify the real structure of BP layer, further information need to be collected and further experiment, like HRTEM or EXAFS, need to be carried out.

Conclusions

BP epitaxial layer grown on 4H-SiC substrate with a 4.37° off-cut angle is characterized by optical microscopy, SWBXT and SEM. The growth orientation is $(111)_{BP}<1\text{-}10>_{BP}||(0001)_{4H\text{-}SiC}<11\text{-}20>_{4H\text{-}SiC}$. The BP layer is dominated by matrix BP, but twin defects also appear in the epitaxial layer. Because although the 4.37° off-cut narrow the terrace, but the width of each step is still wide enough for the possible rotational variants to happen. Thus, the reason for formation of twin defect failure may be the insufficient off-cut angle or the substrate problem. And the antisite point defect has been revealed, but further works need to be done.

3.1.3. Characterization of epitaxial BP grown on 3C-SiC/Si

Outline

Microstructure of BP epitaxial layers grown on 3C-SiC/Si substrates has been studied with optical microscopy and SWBXT. (001) BP structure is shown in x-ray topography Laue

pattern and no BP twin structures are found. The epitaxial relationship is (001)Si<110>Si||(001)3C-SiC<110>3C-SiC||(001)BP<110>BP.

Introduction

Silicon with its low cost and advantages in microelectronic devices is attractive as a choice for subbstrate. However, the large lattice mismatch between BP and Si leads to the poor quality of epitaxial film. So, to solve this problem, using 3C-SiC as a buffer layer becomes a choice, because both the lattice mismatch and the thermal expansion coefficient difference are smaller between 3C-SiC and BP. (Tab.III-1)

Tab. III-1. The properties of BP, SiC and Si

	BP	**Si**	**3C-SiC**	**6H-SiC**
Lattice constant(Å)	a=4.54	a=5.43	a=4.36	a=3.08 c=15.12
Coefficient of Thermal expansion (10^{-6} K^{-1})	3.6	2.6	3.3	3~5

Many research has been carried out on GaN or ZnO grown on 3C-SiC/Si and have proven the success of this method[24]. For BP epitaxial growth, this research is just being initiated. For this study, the basic characterization, like orientation identification and twin structure, has been analyzed. And since silicon and 3C-SiC are cubic structure, so the growth direction for BP film is different from the growth on 4H-SiC, which is (001)Si<110>Si||(001)3C-SiC<110>3C-SiC||(001)BP<110>BP. And also, the four fold symmetry structure, in principle, will not cause twin defects, because the 180° rotation about [001] axis will exhibit no difference from the matrix structure.

Results and Discussion

For the growth of BP films on 3C-SiC/Si, the substrate is on axis and the orientation information has been determined by SWBXT technique (Fig.III.11(b)). By optical observation of BP layers, the wide spread square features have been clearly shown on Fig.III.11(a). There exist no BP twin features in the image.

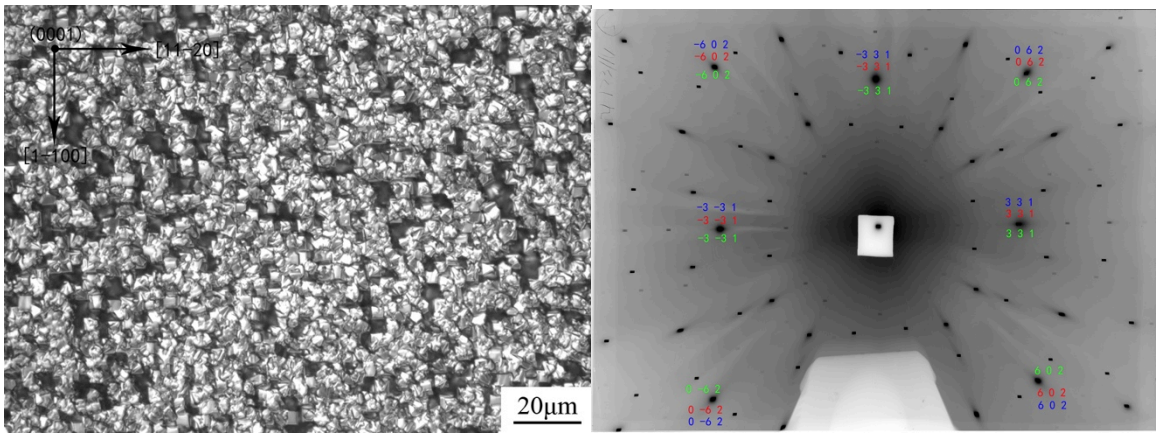

(a) (b)

Fig. III.11. (a)The optical image of BP layer; (b) The diffraction pattern got from SWBXT

The Miller indices of spots have been marked in Fig.III.11 (b). Since the diffraction spots from 3C-SiC and BP are almost same, which means the source of strain points can hardly separate whether from BP or 3C-SiC, but normally, the buffer layer should be quite thin and 3C-SiC will be well-defined square spots, so the major source of blurring should come from BP layer. For relative intensity contrast, silicon Laue pattern satisfy the standard relative intensity, which means the strong spots shows higher contrast while the weak spots represent lower contrast. Meanwhile, all the strain spots obey the high intensity diffraction spots of BP, which means the interfacial stress is quite high. Because the mismatch between the film and substrate causes the distortion of lattice (Fig.III.12) Based on the intensity comparison, antisites defects do appear to be present for the growth of BP on 3C-SiC/Si substrates.

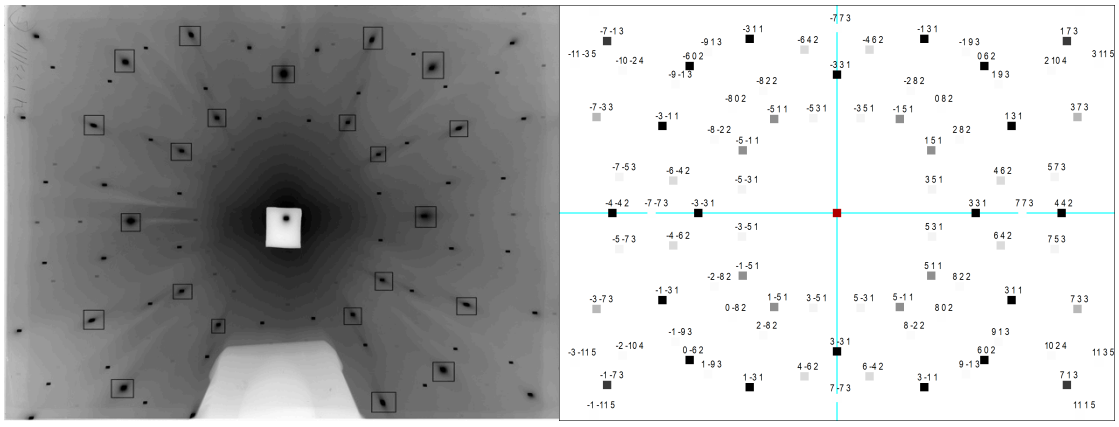

(a) (b)

Fig. III.12. (a) The high blurring spots marked in SWBXT pattern; (b) the standard Laue pattern

Conclusions

BP epitaxial layer grown on 3C-SiC/Si substrate is characterized by optical microscopy and SWBXT. The growth orientation determined by SWBXT, is $(001)_{BP}<110>_{BP}||(001)_{3C\text{-}SiC}<110>_{3C\text{-}SiC}||(001)_{Si}<[110]_{Si}$. The BP layer is dominated by matrix BP, and no twin defects have been found. Because the cubic structure can hardly offer multiple possible positions for BP to bond with, which reduced the possibility of twin structures. No anti-sites point defects have been found based on SWBXT diffraction pattern.

3.1.4 Characterization of epitaxial BP grown on AlN/Sapphire

Outline

Microstructure of BP epitaxial layers grown on AlN/Sapphire substrates has been characterized by optical microscopy and SWBXT. Matrix and twin boron phosphide have been revealed. And the thicker the epilayer, the stronger shadow of Laue pattern shown in x-ray topography. And $(0001)_{Al2O3}<1\text{-}100>_{Al2O3}||(0001)_{AlN}<11\text{-}20>_{AlN}||(111)_{BP}<1\text{-}10>_{BP}$ is the epitaxial relationship.

Introduction

Sapphire substrates have been widely used for the growth of BP films, but because of the high mismatch and high thermal expansion coefficient difference, the quality of BP films grown on sapphire substrate is poor. Therefore, to solve this problem, Aluminum nitride (AlN) film is deposited on sapphire substrate as the buffer layer. Many researches have proved that the advanced AlN/Sapphire substrate offers a great opportunity for GaN epilayer to grow[11.12]. Since AlN (0001) plane is six fold symmetry, so the possibility of structural variants has increased, which is similar to the growth of BP film on 4H-SiC. And in this study, by using different reaction time, the relationship between the thickness of BP films and the contrast of strain spots has been analyzed by SWBXT. In this chapter, the detail analysis of BP twin structure has been studied and the reaction conditions has been taken into consideration.

Results and Discussion

For the growth of BP films on AlN/Sapphire, the substrate has no off-cut and the orientation information has been determined by SWBXT technique (Fig.III.14). By optical observation of BP layers, the equilateral triangle patterns have been clearly shown on Fig.III.13. There exist two kinds of equilateral triangle that relatively rotated by 180° about the [111] BP surface normal, which means the matrix and twin BP structure.

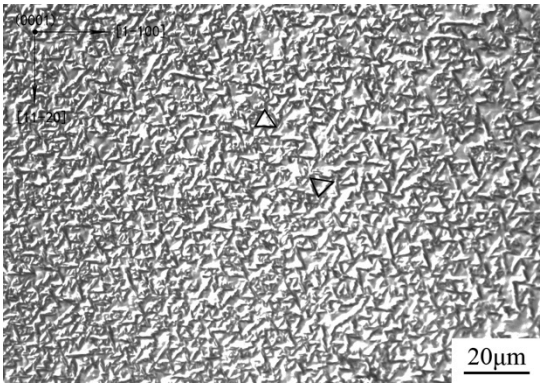

Fig. III.13. The optical image of BP layer shows the two directions of triangle

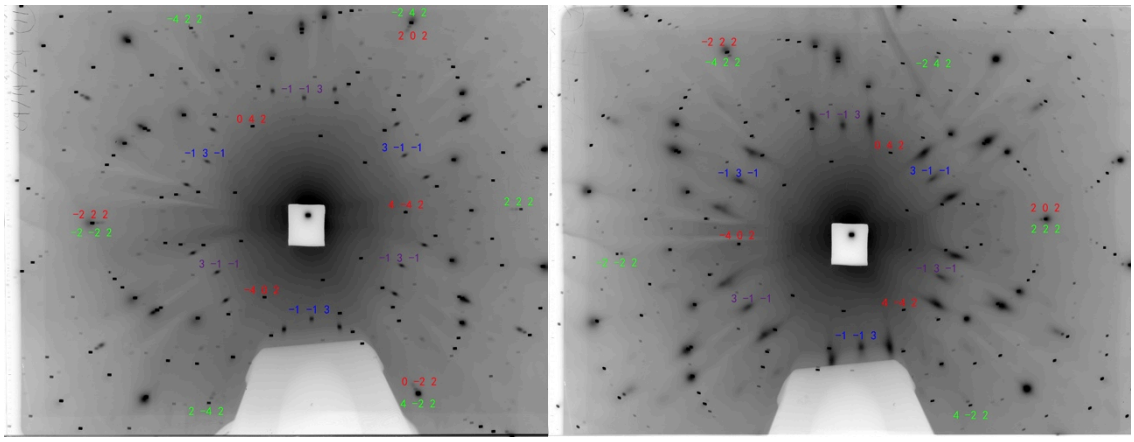

(a) (b)

Fig. III.14 (a) sample with shorter reaction time; (b) sample with longer reaction time

Fig.III.14 mark the diffraction spots from different materials and different planes: red represents the projection of (0001)Al_2O_3<1-100>Al_2O_3; green represents the projection of (0001)AlN<11-20>AlN; blue represents the projection of (111)BP<1-10>BP, purple represents the projection of twin (111)BP<1-10>BP. By comparing (a) and (b), the contrast of strain spots is stronger in (b) because of the thicker BP layer. Based on the Tab.III-2 below, the reaction conditions for two samples are different, sample b has longer reaction

time, which caused the film thickness around 10 μm. The thicker film causes stronger effect on interfacial stress between the substrates and film, which shows higher contrast of strain spot on the Laue pattern.

Tab. III-2 Basic condition information for sample a and b

Sample #	Substrate	Reaction conditions	P/B ratio	Remarks
(a)	AlN/Sapphire	1200^{0}C, 1.5 hr	1000	High P/B ratio
(b)		1200^{0}C, 3 hr	100	Longer reaction time. Film thickness ~10 μ

And by detailed analysis of each spot, more information have been revealed. For example, in the Fig.III.15, the blue squares represents diffraction spots from (111)BP<1-10>BP, which shows the three fold symmetry pattern; the red circles represent diffraction spots from (0001)AlN<11-20>AlN, which is six-fold symmetry; the green triangles represent a three-fold symmetry pattern or can be treat as two fold symmetry, however, by comparing with the Laue pattern, they only belong to the $(0001)_{Al2O3}$<1-100>$_{Al2O3}$ diffraction pattern.

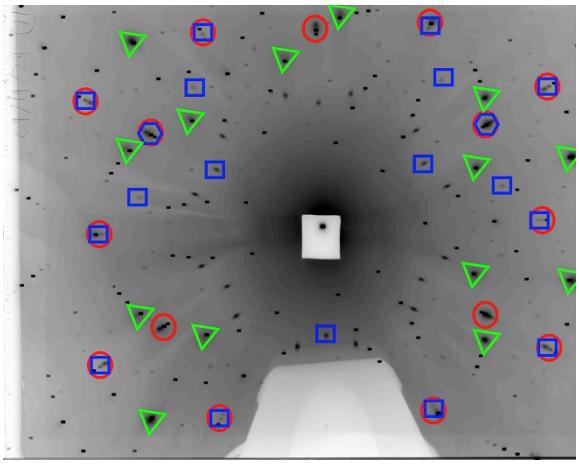

Fig. III.15. Red circles represent AlN; blue squares represent matrix BP spots; blue hexagonal represents the inconsistency intensity of BP; green triangles mark the unknown materials

Based on previous discussion, the blurring spots are formed by the high interfacial

strain between films and substrates, but the blurring green triangles have no match with AlN or BP, which indicates another possible unknown material, such as AlP, BN, and similar materials which is created during the growth process. However, when analyzing the structure of these materials, the results do not match. Another possible reason is, the mismatch of standard Laue pattern and marked triangles is caused by the highly strain, which means the lattice parameter of one layer material has changed. Above all, further analysis and technique need to be carried out.

Also, the analysis of the relative intensities of spots indicates the possible presence of antisites point defects. The blue hexagonal in Fig.III.15 represent the weak intensity spots in standard Laue pattern, however, in real crystal diffraction pattern, the intensity is as strong as other strong spots. This phenomenon is also observed in the growth of BP on 4.37° off-cut c-plane 4H-SiC, which is named as antisites point defects. The defect is caused by the exchange of different materials atoms, the arrangement of atoms has changed, which lead to the inconsistency in the relative intensities of diffraction spots.

To explain the appearance of BP twin, the growth procedure should be modified. The BP epitaxial layer is grown on AlN/sapphire substrate by metal-organic vapor phase epitaxy method. The thin layer of AlN mitigated the high mismatch problem of sapphire and BP, but the six-fold symmetry of AlN (0001) plane. The principle of bonding configuration is similar to the growth of BP films on the 4H-SiC.

Conclusions

BP epitaxial layer grown on AlN/sapphire (AlN use as a buffer layer) substrate is characterized by optical microscopy and SWBXT. The growth orientation is $(111)_{BP}$<1-10>$_{BP}$||||$(0001)_{AlN}$<11-20>$_{AlN}$||$(0001)_{Al2O3}$<1-100>$_{Al2O3}$. The BP layer is dominated by twin BP, which because the buffer layer is six-fold symmetry, which offers more opportunity for BP to bond. And the relationship of film thickness and strain contrast has been analyzed, which shows thicker the film, stronger contrast of the strain spots. Also, based on the comparison between standard Laue pattern and real diffraction pattern, the possible unknown materials have been found, which exhibits strong contrast in blurring. The antisites defects were also found in BP layer.

3.2. Conoscopic Method Analyzing the Defect of Sapphire Wafers

Outline

In this study, two inch sapphire wafers have been studied by polarized optical method and SWBXT. The following work in stress analysis around grain boundaries has been exhibited by the feature change of Maltese cross interference pattern.

Introduction

The two inch sapphire wafers, cut from boules, a HEM method have been analyzed by SWBXT and polarized optical method. Beyond the dislocation density calculation and other characterization, there exist a straight grain boundary line across through the whole sample which needs stress analysis. Normally, polycrystalline solids contain numerous randomly orientated grains separated by grain boundaries, which is described as an array of dislocations. If the orientation difference between the grains is large, the arrangement of atoms in the boundary region will be complicated. Dislocation nets may cause stress field around the grain boundaries, which is sensitive to the Burgers vector, orientation and the arrangement of atoms. And the total stress field should be the combination of single edge and screw dislocations, which lists the stress equation below.[8]

$$\sigma_{xx} = \frac{-Gb}{2\pi(1-v)} \sum_{n=-N}^{N} \frac{y_n(3x^2 + y_n^2)}{(x^2 + y_n^2)^2}$$

$$\sigma_{yy} = \frac{Gb}{2\pi(1-v)} \sum_{n=-N}^{N} \frac{y_n(x^2 - y_n^2)}{(x^2 + y_n^2)^2}$$

$$\sigma_{xy} = \frac{Gb}{2\pi(1-v)} \sum_{n=-N}^{N} \frac{x(x^2 - y_n^2)}{(x^2 + y_n^2)^2}$$

where y_n=y-nD and D is the dislocation spacing.

Polarized optical method with its convenience and reasonable analysis has been a great tool for basic analysis of crystal boule. But in this study, the sample has been sliced into thin wafers, so high magnification (x50) objective lenses are needed. And based on the Maltese cross formation principle, which is a colorful Maltese cross shows when the

polarizer and analyzer are crossed, and its sensitivity in dealing with stress field, the distortion of interference pattern can describe and evaluate the defects of crystal boule.[9]

Results and Discussion

Based on the previous study by SWBXT technique, there exist a low-angle grain boundary in the sample, which may be caused by plastic deformation. (Fig.III.16) When analyzing under the polarized optical microscopy, the deformation of Maltese cross has been revealed. Based on the severity of deformation, the stress of grain boundaries in these samples is acceptable. Fig.III.16 (b) shows the undistorted Maltese cross interference pattern captured from the grain boundary free zone.

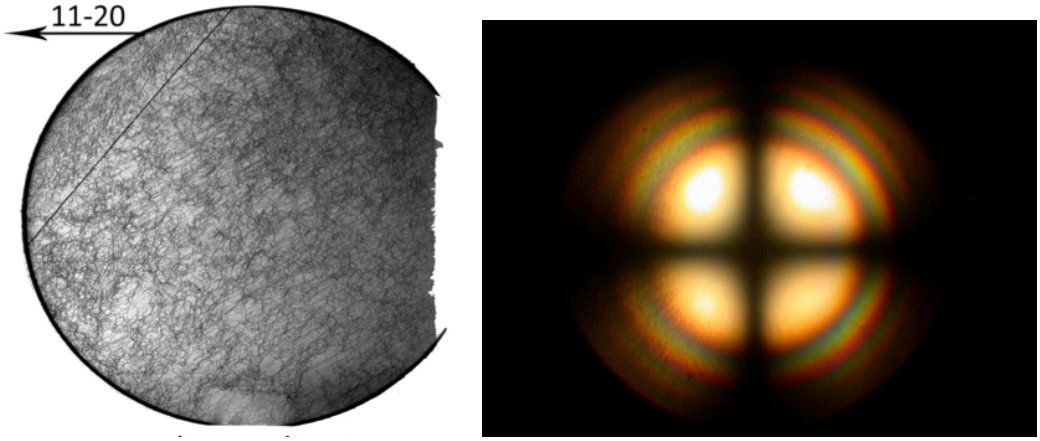

(a) (b)

Fig. III.16. (a) The topography image of sample; (b) undistorted Maltese cross interference pattern

When the polarized light source crosses the straight grain boundary line, the fringes and center cross are distorted, and also, the curve features shows opposite shape when compared above the line with that below. Fig.III.17 shows several conoscopic patterns along the line when passing across the line.

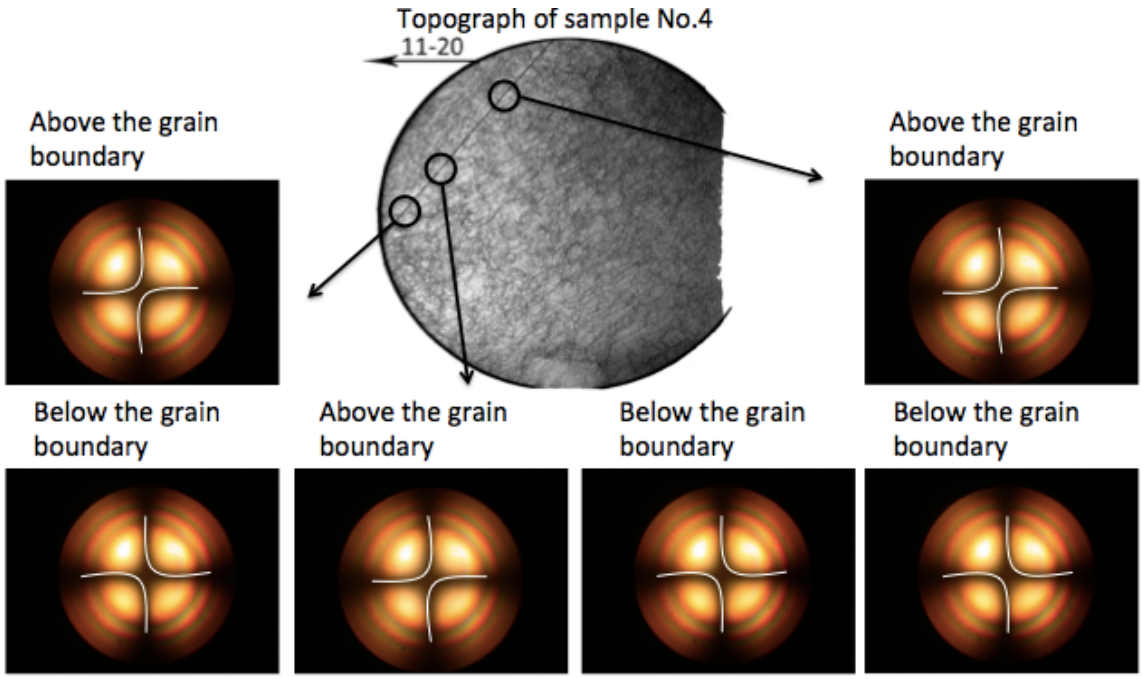

Fig. III.17. The conoscoppic pattern of three different spots along the grain boundaries

The conoscopic pattern is obtained by overlapping five sapphire wafers together with same orientation, because the magnification is not sufficient enough to form the Maltese cross pattern, to solve this problem, increasing the thickness of sample, which means overlapping more wafers, is an easy and quick way to achieve it.

Based on the information from Fig.III.17, the deformation of Maltese cross can only be captured around the grain boundary line, which means the remaining area has no stress or weak stress influence. For the line area, there exists a common phenomenon for this sample: all the shapes of cross above the line area are same and opposed to the pattern below the line, which means the distribution map of stress field has relationship with the location of sample. So, if we assume the stress above the line exhibits positive, then the stress below the line appears as negative，which might also be explained as one side is dominated by tension, the other side is dominated by compression. So as the polarized light passing the line, the pattern's direction of distortion also changes immediately.

To confirm this phenomenon, two other sets of sapphire wafers have been reviewed and similar results were obtained (Fig.III.18 and Fig.III.19).

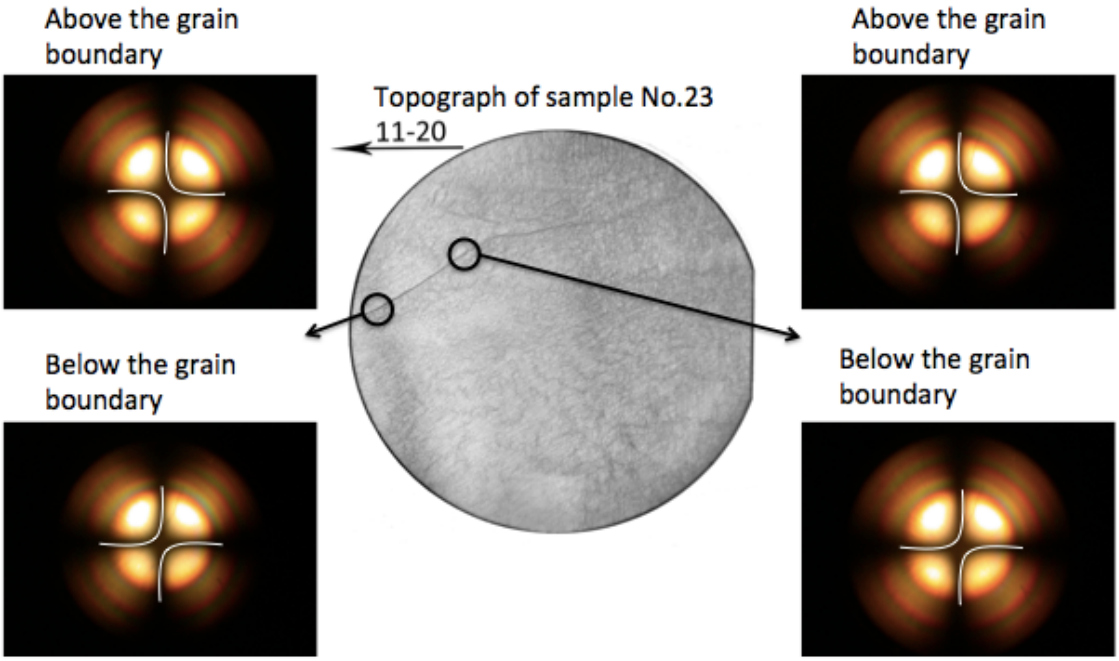

Fig. III.18. The Maltese cross pattern of second set of sample

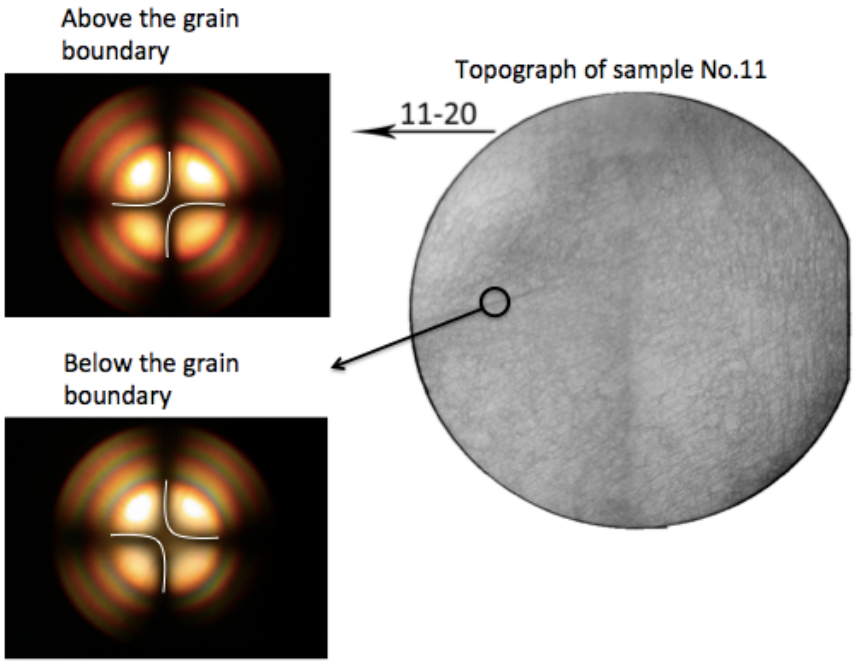

Fig. III.19. The Maltese cross pattern of the third set of sample

As pictured in Fig.III.18 and Fig.III.19, this phenomenon is also visible in these two sets of samples. However, the curve pointing direction are not same, for example, in Fig.III.18,

when polarized light sitting above the line, the cross pattern is same as the below-line pattern of Fig.III.17, and vise versa. This shows that the cross curve direction will change if the stress field changed, which means maybe the stress field of the second set of wafers is opposite to the first set. However, the Fig.III.19 shows the same stress distribution as the first set of sample，which means the stress field of third set of wafers is same as the first one.

The polarized optical microscopy only offers a relative evaluation of samples, and since the overlapping samples cannot accurately represent the properties of one single wafer, which means the mismatch error of orientation of five bonded samples is inevitable, and the dependence of the distortion of Maltese cross on it needs to be considered.

Conclusions

By using polarized optical microscopy, the Maltese cross interference pattern of sapphire wafer has been analyzed. The distortion of center cross occurs across the grain boundary line area, while the remaining wafer areas are shows perfect well-defined cross shape and fringe. When the polarized light source passing across the grain boundary line, the center cross shape changes immediately. And the cross shapes above the line are same, so are the shapes below the line, but the relationship between the above and below is opposite, which may cause by the different stress field distribution. Further analysis of the relationship between the deformation of Maltese cross and the stress field distribution needs to be continued.

CHAPTER.IV. CONCLUSION AND DISCUSSIONS

Defect characterization of BP grown on 4.37° off-cut c-plane 4H-SiC, AlN/sapphire and 3C-SiC/Si substrates have been analyzed by SWBXT, SEM and optical microscopy method.

First, SWBXT, optical microscopy and SEM 6H-SiC have been used to characterize the growth BP layer on c-plane. The SWBXT technique has determined the epitaxial relation, which is $(111)_{BP}\langle 1\text{-}10\rangle_{BP}||(0001)_{6H\text{-}SiC}\langle 11\text{-}20\rangle_{6H\text{-}SiC}$. The BP layer is dominated by twin structures, which is caused by the wide bonding platform on substrates.

Second, the epitaxial relation between BP layer and 4.37° off-cut c-plane 4H-SiC substrate has been determined as $(111)_{BP}\langle 1\text{-}10\rangle_{BP}||(0001)_{4H\text{-}SiC}\langle 11\text{-}20\rangle_{4H\text{-}SiC}$ by SWBXT technique. Both the matrix and twin structures have been reviewed by optical microscopy and SEM, which presents two kinds of triangle, relatively rotated by 180°. The x-ray topography also proved the existence of twin structures and revealed that the BP layer is mainly dominated by matrix orientation. Also, using the Crystal Maker software, the off-cut surface structure of 4H-SiC has been built, and by bonding BP (111) plane structure with the terrace, the possibility of bonding configuration shows that the terrace is wide enough to be deposited, which leads to the appearance of twinned orientation BP. And by comparing the relative intensity of each point, the antisites point defects have been found. To further identification of crystal structure, TEM and other technique should be applied.

Third, based on the large lattice constant difference of BP and Si, the growth of BP epilayer on Si substrate has always been a problem. In this study, we use 3C-SiC materials as a buffer layer to reduce the mismatch between silicon and boron phosphide, because 3C-SiC has closer lattice constant and thermal expansion coefficient with BP compared to Si. The epitaxial relationship has been examined by SWBXT, which is $(001)_{Si}\langle 110\rangle_{Si}||(001)_{3C\text{-}SiC}\langle 110\rangle_{3C\text{-}SiC}||(001)_{BP}\langle 110\rangle_{BP}$. Since the structure of silicon is cubic, which also worked for 3C-SiC and BP, so the symmetry is four-fold, which means in principle there exist no possibility to grow twin structure. And the relative intensities of blurring spots are same as the standard Laue pattern, but the source of blurring can hardly be identified. No twin defects have been revealed.

Fourth, for the growth of BP layer on AlN/sapphire substrate, the epitaxial relationship is $(0001)_{Al2O3}\langle 1\text{-}100\rangle_{Al2O3}||(0001)_{AlN}\langle 11\text{-}20\rangle_{AlN}||(111)_{BP}\langle 1\text{-}10\rangle_{BP}$. Also, since there is a high mismatch in lattice constant and thermal expansion coefficient between sapphire and BP, the thin film of AlN acts as a buffer layer to reduce this problem. The twin structure has

been reviewed clearly from optical microscopy, two kinds of triangle relatively rotated by 180°. The SWBXT also proved the high contrast blurred spots are from both BP layer and AlN buffer layer, which means the interfacial stress between the three layers is quite high. And the relationship between thickness and blurred contrast is observed. Diffraction pattern from an unknown material has also been revealed, the high contrast blurred spots show the possible high interfacial strain between the unknown layer and substrates.

Lastly, the stress field of sapphire wafers has been analyzed by polarized optical microscopy. The deformation of Maltese cross interference pattern shows the stress distribution around the grain boundary area. And the center cross shape changes immediately when polarized light passing across the grain boundary line. All the patterns are same on one side of the line, which means the stress distribution is constant on one side of the line and opposite to the other side of line.

CHAPTER.V. FUTURE WORK

The defect analysis of BP grown on different types of substrates, and for each kind of substrate, major issues need to be addressed. For example, for 4H-SiC substrate, in principle, the off-cut angle, which narrows the width of platform, should reduce the possibility of structural variants. However, the influence of off-cut process is weak, so further structural optimization should be researched, like other choice of substrates.

And for AlN/sapphire substrates, the presence of twins in BP layer means the AlN buffer layer brings more options for structural variants. And the interfacial stress between AlN and sapphire is also very large, which needs to be analyzed whether it will bring further influence the epitaxial layer growth. And the sources of some blurring spots have not been identified which needs to be examined. For the growth of BP epilayer on 3C-SiC/Si substrate, the quality of BP layer is acceptable, and no twin or structural variants have been revealed. However, further proof need to be collected.

For the conoscopic pattern, the unavoidable error when dealing with the overlapping wafers needs to be diminished by using higher magnification lens or changing wafers to sapphire boule. And we need to simulated the stress filed around grain boundary area.

REFERENCE

1. Nina Hong, John Mullins, Keith Foreman and S Adenwalla, “Boron carbide based solid state neutron detectors: the effects of bias and time constant on detection efficiency”, J. Phys. D: Appl. Phys. 43 (2010) 275101 (11pp)
2. Ugochukwu Nwagwu,” FLUX GROWTH AND CHARACTERISTICS OF CUBIC BORON PHOSPHIDE”, master thesis of Kansas State University
3. Guoliang Li, “Growth and Properties of Boron Phosphide Films on Silicon Carbide”, doctoral dissertations of University of Tennessee
4. Huili Tang, Hongjun Li and Jun Xu, “Growth and Development of Sapphire Crystal for LED Applications”, Advanced Topics on Crystal Growth
5. Balaji Raghothamachar,* Govindhan Dhanaraj, Jie Bai, and Michael Dudley, “Defect Analysis in Crystals Using X-ray Topography”, Microscopy Research and Technique 69:343-358 (2006).
6. Joseph I. Goldstein, Dale E. Newbury, Patrick Echlin, David C.Joy and etc., “Scanning Electron Microscopy and X-ray Microanalysis (third edition)”, Kluwer Academic/Plenum Publishers
7. “LEO 1550 Scanning Electron Microscope manual”, Marvell Nanofabrication Laboratory
8. D. Hull and D. J. Bacon, “Introduction to Dislocations (Fourth Edition)”, Butterworth-Heinemann
9. O. Yu. Pikul’, K. A. Rudo , and V. I. Stroganov, “Features of the formation of a Maltese cross in conoscopic patterns”, Opticheski Zhurnal **75**, 84–87 (July 2008)
10. Marek Niewczas, “Dislocations and Twinning in Face Centred Cubic Crystals”, Dislocations in Solids, 2007 Elsevier B.V.
11. Masahira Sakai, Hiroyasu Ishikawa, Takashi Egawa, and etc.,” Growth of high-quality GaN films on epitaxial AlN/sapphire templates by MOVPE”, Journal of Crystal Growth 244 (2002) 6-11
12. Makoto Miyoshi, Takashi Egawa, Hiroyasu Ishikawa, and etc., “Nanostructural characterization and two-dimensional electron-gas properties in high- mobility Al GaN AlN GaN heterostructures grown on epitaxial AlN/sapphire templates”, Journal of Applied Physics 98, 063713 (2005)
13. X.Song, J. F. Michaud, F. Cayrel, M. Zielinski, M. Portail, and etc.,” Evidence of electrical activity of extended defects in 3C–SiC grown on Si”, Applied Physics Letters 96, 142104 (2010)
14. Yoshihisa Abe, Jun Komiyama, Syunichi Suzuki, Hideo Nakanishi, “SiC epitaxial growth on Si(0 0 1) substrates using a BP buffer layer”, Journal of Crystal Growth 283 (2005) 41–47
15. C. P. Flynn and J. A. Eades, Thin Soild Films, 389, 116 (2001)
16. M. Dudley, X. R. Huang and W. Huang, J. Phys. D: App. Phys., 32, A139 (1999)

17. D. Emin and T. L. Aselage, J. App. Phys., 97, 013529 (2005)
18. G. A. Slack, D. W. Oliver and F. H. Horn, Phys. Rev. B, 4, 1714, (1971)
19. 29 J. Takahashi, N. Ohtani, M. Katsuno, and S. Shinoyama, J. Crystal Growth., 181, 229 (1997)
20. H. Chen, G. Wang, M. Dudley, L. Zhang, L. Wu, Y. Zhu, Z. Xu, J.H. Edgar and M. Kuball, J. Appl. Phys., 103 (12), (2008)
21. Popper, P.; Ingles, T. A. Boron phosphide, a III–V compound of zinc-blende structure. Nature 1957, 179, 1075–1075
22. Kumashiro, Y. Refractory semiconductor of boron phosphide. Journal of Materials Research 1990, 5, 2933–2947
23. Govindhan Dhanaraj, Kullaiah Byrappa, Vishwanath Prasad, Michael Dudley, "Handbook of Crystal Growth", Springer Heidelberg Dordrecht London New York, ISBN: 978-3-540-74182-4.
24. Tetsuya Takeuchi, Hiroshi Amano, Kazumasa Hiramatsu, Nobuhiko Sawaki, Isamu Akasaki, "Growth of single crystalline GaN film on Si substrate using 3C-SiC as an intermediate layer" Journal of Crystal Growth, Volume 115, Issues 1-4, 2 December 1991, Pages 634 – 638